Wavelet-Based Adaptive Solution for the Nonuniform Multiconductor Transmission Lines

S. Grivet-Talocia and F. Canavero, *Member, IEEE*

***Abstract*—A time-domain technique for the solution of arbitrary nonuniform multiconductor transmission lines (NMTL's) is presented. The technique is based on a weak formulation of the NMTL equations obtained through spatial expansion of the voltage and current vectors into biorthogonal wavelet functions. Wavelets allow adaptive representations of the solution by using few expansion coefficients, with any fixed approximation order. The set of significant expansion coefficients is determined automatically from the solution, which can be computed very efficiently. A numerical example illustrates the high adaptivity of the method.**

***Index Terms*—Distributed parameter circuits, multiconductor transmission lines, time domain analysis, wavelet transforms.**

I. Introduction

MANY interconnections of practical interest are characterized by cross sections which are not translation-invariant. Examples can be impedance matching networks or cables in complex geometries, like automobiles or airplanes. The nonuniform multiconductor transmission lines (NMTL's) represent a good model for the simulation of the electrical behavior of these structures, avoiding the need for full-wave simulations based on method of moments (MoM), finite difference time domain (FDTD), or finite-element method (FEM). This applies of course only when the longitudinal variations are not too large, so that the quasi-TEM mode assumption remains applicable.

This letter presents a novel method for the transient simulation of arbitrary lossy NMTL structures. The method is based on a weak formulation of the NMTL equations, which leads to a class of numerical schemes of different approximation order according to the particular choice of some trial and test functions. We will use wavelet functions because the waveforms of high-speed digital signals can be represented with small approximation errors and very few expansion coefficients in a wavelet basis. The optimal sparsity of wavelet representations is indeed a well-known result from the theory of nonlinear approximations [1]. As the spatial domain is intrinsically bounded, we will use biorthogonal boundary adapted wavelets constructed from B-spline functions. The details of this construction can be found in [2], while the main properties are listed in the next section.

The main advantage of the numerical scheme is that the representation of the solution is automatically adapted when time advances. Given a fixed accuracy, the solution is stored with the fewest possible wavelet expansion coefficients, which are the only ones used for the actual calculations. This results in a small computational effort in the determination of the solution compared to intrinsically nonadaptive methods like FDTD. In addition, the weak formulation of the NMTL equations allows the treatment of arbitrary lines with even varying phase speed. The accuracy of other methods like FDTD is severely limited for such structures by numerical dispersion.

Manuscript received April 3, 1998.

The authors are with the Dipartimento di Elettronica, Politecnico di Torino, 10129, Torino, Italy.

Publisher Item Identifier S 1051-8207(98)05696-7.

II. Wavelet Basis

Given a function $v \in L^2$ defined on a domain $\Omega \subseteq \boldsymbol{R}$, we can introduce a sequence of approximation spaces

$$V_{j_0} \subseteq \cdots \subseteq V_j \subseteq V_{j+1} \subseteq \cdots \subseteq V_J \subseteq L^2$$

indexed by a *refinement level* j. Increasing values of j define better and better approximations v_j of the initial function v. In the following, the levels j_0 and J define the coarsest and finest approximations, respectively.

The basic idea behind wavelets is to express the approximation v_J through a *hierarchical* representation, obtained by decomposing the space V_J into a coarse approximation space V_{j_0} plus some detail spaces W_j:

$$V_J = V_{j_0} \oplus \bigoplus_{j=j_0}^{J-1} W_j. \tag{1}$$

The basis functions ψ_{jk} of these detail spaces W_j are called *wavelets*, while the basis functions φ_{jk} of the approximation spaces V_j are called *scaling functions*. Note that these functions are labeled by two indexes, the first representing the refinement level and the second distinguishing different functions at the same level.

The advantage of this decomposition is that a good approximation of v can be obtained by simply adding to a coarse approximation v_{j_0} some detail functions. However, not all the details need to be added, but only those leading to an improvement in the approximation error. The theory shows that the location and the number of needed details can be automatically determined by looking at the magnitude of the wavelet expansion coefficients. In summary, we will use the representation

$$v \simeq \sum_k c_{j_0,k}\varphi_{j_0,k} + \sum_{j=j_0}^{J-1} \sum_k w_{jk}\psi_{jk} \tag{2}$$

1051–8207/98$10.00 © 1998 IEEE

where few coefficients w_{jk} are effectively used in the superposition. The cutoff criterion is absolute thresholding, i.e., a term is retained only if $|w_{jk}| > \epsilon$. The particular value of ϵ tunes the accuracy of the representation.

The scaling functions and wavelets can be orthogonal, with the decomposition of (1) obtained through orthogonal sums. This setting is widely used in the literature [3]. However, it can be shown that orthogonal wavelets cannot be at the same time symmetric and compactly supported [4]. Symmetry is convenient for the implementation of numerical schemes, while a compact support is essential when complicated boundary conditions are to be enforced. These two features can be recovered if orthogonality is released in favor of the more general bi-orthogonality [4]. This requires to introduce dual scaling functions $\tilde{\varphi}_{jk}$ and wavelets $\tilde{\psi}_{jk}$, mainly used for the computation of the expansion coefficients in (2).

III. Mathematical Formulation

Let us consider the NMTL equations

$$\begin{aligned}\frac{\partial}{\partial z}\boldsymbol{V}(z,t) &= -\boldsymbol{L}(z)\frac{\partial}{\partial t}\boldsymbol{I}(z,t) - \boldsymbol{R}(z)\boldsymbol{I}(z,t)\\ \frac{\partial}{\partial z}\boldsymbol{I}(z,t) &= -\boldsymbol{C}(z)\frac{\partial}{\partial t}\boldsymbol{V}(z,t) - \boldsymbol{G}(z)\boldsymbol{V}(z,t)\end{aligned} \tag{4}$$

with $\boldsymbol{V}(z,t)$ and $\boldsymbol{I}(z,t)$ indicating the voltage and current vectors at location z and time t. The line is assumed to have $P+1$ conductors, and the per-unit-length parameters $\boldsymbol{L}(z), \boldsymbol{C}(z), \boldsymbol{R}(z)$, and $\boldsymbol{G}(z)$ are $P \times P$ matrices whose entries are arbitrary functions of the space variable z. Without loss of generality we will consider the length of the line to be normalized, i.e., $z \in [0,1]$. For simplicity, the line is supposed here to be terminated by Thévénin loads

$$\begin{aligned}\boldsymbol{V}(0,t) &= \boldsymbol{V}_S(t) - \boldsymbol{R}_S\boldsymbol{I}(0,t)\\ \boldsymbol{V}(1,t) &= \boldsymbol{V}_L(t) + \boldsymbol{R}_L\boldsymbol{I}(1,t).\end{aligned} \tag{5}$$

The approximate voltages and currents along the line are sought for in terms of expansion coefficients in the hierarchical basis functions of (2). We collect all these coefficients into the vector $\boldsymbol{x}(t)$. Testing the equations with the dual scaling functions $\{\tilde{\varphi}_{j_0,k}\}$ and wavelets $\{\tilde{\psi}_{jk}\}$ leads to a set of ODE's representing the spatial discretization of the original NMTL equations. A straightforward substitution allows to incorporate the load equations (5) in the system by eliminating the border voltage coefficients in favor of the border current coefficients. This operation is only possible when the basis functions are boundary adapted [5]. The final system of ODE's, after explicitation of the time derivatives, reads

$$\frac{d}{dt}\boldsymbol{x}(t) = \boldsymbol{\Phi}\boldsymbol{x}(t) + \boldsymbol{\Gamma}_S\boldsymbol{V}_S(t) + \boldsymbol{\Gamma}_L\boldsymbol{V}_L(t). \tag{6}$$

This can be solved with a suitable integration method. We used here a fifth-to-sixth-order Runge–Kutta scheme [6].

The typical structure of the system matrix $\boldsymbol{\Phi}$ is depicted in Fig. 1. This matrix is highly sparse. In addition, the array $\boldsymbol{x}$ is also highly sparse, because many of the wavelet coefficients result below the threshold ϵ and are disregarded. Therefore, the product $\boldsymbol{\Phi x}$ can be computed very efficiently with an optimized code.

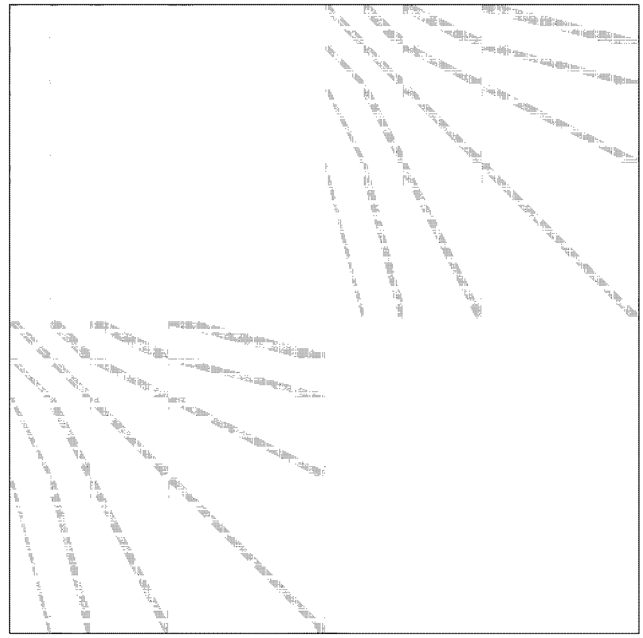

Fig. 1. Structure of the system matrix $\boldsymbol{\Phi}$ stemming from the wavelet spatial discretization of the NMTL equations.

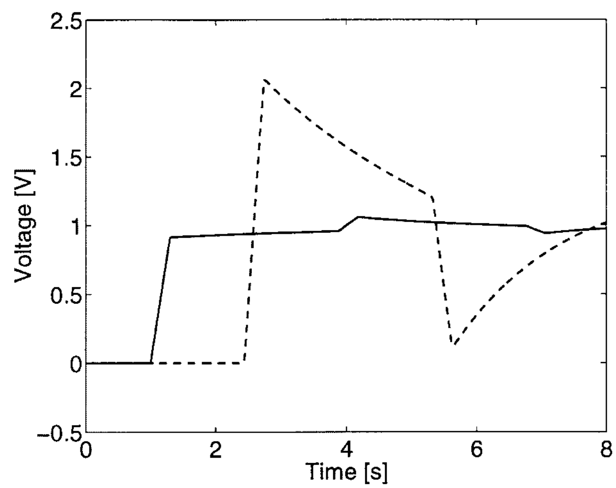

Fig. 2. Voltage at the left (solid line) and right (dashed line) terminations of a line with exponentially decreasing phase speed.

IV. Numerical Results

A validation of the TDSE method through a detailed analysis of the approximation errors can be found in [5] and [7], and will not be repeated here. This section shows instead the simulation of a lossless line with nonuniform propagation speed in order to point out the high adaptivity of the proposed scheme. The (normalized) per-unit-length parameters are as follows:

$$L(z) = 4^z \text{ H/m}, \qquad C(z) = 1 \text{ F/m}.$$

These parameters lead to an exponentially increasing nominal characteristic impedance (from 1 up to 2 Ω) and to an

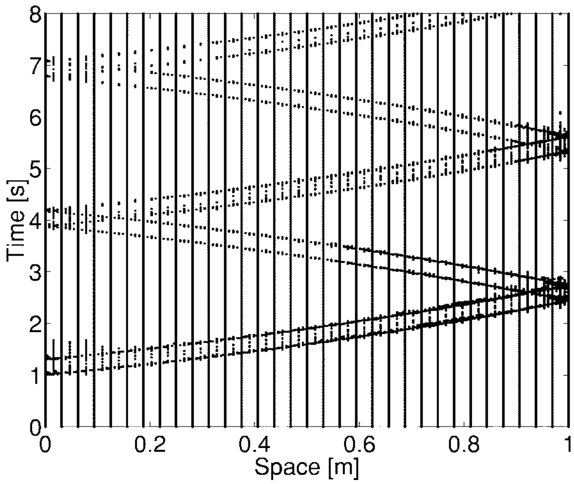

Fig. 3. Location of the significant voltage wavelet coefficients for a line with exponentially decreasing phase speed.

exponentially decreasing nominal phase speed

$$\nu(z) = \frac{1}{\sqrt{L(z)C}}.$$

We consider a nonmatched line with nominal reflection coefficients at the left and right ends equal to $\Gamma_S = -9/11$ and $\Gamma_L = 2/3$, respectively. With these load conditions, the input voltage pulse undergoes significant reflections at the line ends. The voltage waveform used in the following is a 1-V step function with rise time equal to 0.3 s. The resulting voltages at the left and right terminations are plotted in Fig. 2, while the location of the significant wavelet coefficients (using a threshold $\epsilon = 10^{-4}$) is plotted in Fig. 3. It should be noted that these coefficients trace the characteristic curves of the transmission line equations, tracking the location of the singularities (i.e., the points where the derivative of voltage and current is discontinuous). These curves are significantly bent, with a tangent at a fixed z equal to $\pm 1/\nu(z)$. The figure clearly shows the sparsity in the overall representation of the solution and the high adaptivity of the method.

References

[1] R. A. DeVore, B. Jawerth, and V. A. Popov, "Compression of wavelet decompositions," *Amer. J. Math.*, vol. 114, pp. 737–785, 1992.

[2] L. Levaggi and A. Tabacco, "Wavelets on the interval and related topics," Dept. Mathematics, Politecnico di Torino, Italy, Rep. no. 11-1997.

[3] L. Katehi and M. Krumpholz, Eds., *Special Issue on Wavelets in Electromagnetics*, *Int. J. Num. Model.*, vol. 11, pp. 1–96, 1998.

[4] A. Cohen, I. Daubechies, and J. Feauveau, "Biorthogonal bases of compactly supported wavelets," *Comm. Pure Appl. Math.*, vol. 45, pp. 485–560, 1992.

[5] S. Grivet-Talocia, "Wavelet-based numerical methods for the solution of the Nonuniform Multiconductor Transmission Lines," Ph.D. dissertation, Dept. Electronics, Politecnico di Torino, Italy, 1998.

[6] *IMSL MATH/LIBRARY User's Manual, Version 2.0*, 1991, IMSL, Houston, TX.

[7] S. Grivet-Talocia and F. Canavero, "Weak solution of the nonuniform multiconductor transmission lines," presented at the IEEE 1998 Int. Symp. on Electromagnetic Compatibility, Aug. 23–28, 1998, Denver, CO.